Supporting Information

Modulation of conformational equilibrium by phosphorylation underlies the activation of deubiquitinase A

Ashish Kabra, Efsita Rumpa, and Ying Li*

Department of Chemistry, University of Louisville, 2320 South Brook Street, Louisville, KY 40208

*To whom correspondence should be addressed: E-mail: ying.li.1@louisville.edu

Supporting Methods

CLEANEX experiment

The water exchange rates of backbone amide protons were measured using the phase-modulated CLEAN chemical exchange (CLEANEX-PM) pulse sequence (1). The experiments were performed at 299.6 K on a [^{2}H,^{15}N]-labeled p-DUBA sample at 420 μM in a buffer containing 50 mM sodium phosphate, pH 7.02, 100 mM NaCl and 2 mM TCEP. A series of 2D spectra with transfer periods of 5, 10, 15, 20, 25, 30, 40 and 50 ms and a reference spectrum were acquired. The spin-locking field during the CLEANEX period was 6.3 kHz. Each 2D spectrum was acquired with 1024 (^{1}H) × 180 (^{15}N) complex points and an interscan delay of 2 s. With 36 scans per FID, the total measurement time was approximately 62 h for the complete set. The reference spectrum was acquired with 8 scans. The exchange rate constant (k) was derived from fitting data to the equation below or a linear model when the build-up curves are in the initial rate regime:

$$\frac{I}{I_o} = \frac{k}{(R_{1A,app} + k - R_{1B,app})} \times \{exp(-R_{1B,app}\tau_m) - exp[-(R_{1A,app} + k)\tau_m]\}$$

where k is the rate constant; τ_m is the mixing time; $R_{1A,app}$ is the apparent relaxation rate of the amide ^{1}H during the mixing period. $R_{1B,app}$ is the apparent solvent relaxation rate that was measured by a separate experiment using the same pulse sequence without water suppression, from which the water decay rate during the CLEANEX period was calculated. The value of $R_{1B,app}$ was determined to be 0.6 s^{-1} and the degree of water saturation was determined to be 79% according to the previously described methods (1). The exchange rates for amide protons were corrected by dividing the k by 0.79 due to this effect.

^{15}N transverse relaxation experiment

^{15}N transverse relaxation rates (R_2) were measured on [^{2}H,^{15}N]-labeled wild-type p-DUBA at 500 μM and np-DUBA at 575 μM and 297.6 K in the NMR buffer. The experiments were performed using a modified version of a TROSY-detected pulse sequence (2) . The water magnetization was dephased at the beginning of the ^{15}N relaxation period. The data were acquired using 16 scans for each FID and a recycle delay of 1.5 s in an interleaved fashion. ^{1}H and ^{15}N 90° pulse widths were 10.4 μs and 29.3 μs, respectively, at full power levels. During the R_2 relaxation period, the ^{15}N π pulses were applied every 1.25 ms at the full power level. R_2 values were determined using relaxation delays of 10, 30, 50 and 70 ms. 1024 (^{1}H) × 260 (^{15}N) complex points were recorded for each spectrum with the spectral widths of 11574 Hz in t_2 (^{1}H) dimension and 2695 Hz in t_1 (^{15}N) dimension, respectively.

The ^{15}N transverse relaxation rates were determined by fitting the data to the equation:

$$I(t) = I_0\ e^{-R_2 t}$$

where I_0 is the cross-peak intensity at the zero relaxation delay and $I(t)$ is the intensity at time t.

pH titration experiments

The experiments were carried out on samples of ^{15}N-labeled p-DUBA using buffers containing 50 mM HEPES, 100 mM NaCl and 2 mM TCEP. 1 mM imidazole and 1 mM Tris were added to the samples as internal pH indicators (3). The samples were dialyzed against the buffers at the desired pH values. The sample concentrations were 460-750 μM. Phosphorus 1D experiments were performed at 299.6 K on a Varian Inova-500 MHz spectrometer equipped with a room temperature BBI probe. 17600 scans were recorded for each spectrum with an interscan delay of 2 s. WALTZ16 ^{1}H decoupling centered at 4.3 ppm was applied during the acquisition period. The spectra were indirectly referenced with DSS using the ratio 0.404807210 (4).

^{1}H-^{15}N TROSY experiments were performed on the same set of samples at 299.6 K. Each TROSY spectrum was acquired with 1024 (^{1}H) × 260 (^{15}N) complex points and 8 scans per FID. ^{31}P and ^{1}H chemical shifts of pS177 at various pH values were fit to the equation (5):

$$\delta_{obs} = \left(\delta_{deprot} - \delta D\right) + \frac{\delta D}{1 + 10^{(pK_a - pH)}}$$

where δ_{obs} is the observed chemical shift in ppm, δ_{deprot} is the chemical shift of the deprotonated species, and δD is the chemical shift difference between the protonated and deprotonated species. δD was set to 3.9 ppm for ^{31}P and 0.64 ppm for ^{1}H (6) to fit the titration curves.

^{15}N-NOESY-HSQC experiment

3D ^{15}N-NOESY-HSQC experiment was performed on ^{15}N-labeled p-DUBA at 500 μM in the NMR buffer at 300 K. The data were acquired with a mixing time of 100 ms, 140 complex points in the t_1 period (^{1}H), 48 complex points in the t_2 period (^{15}N), and 1024 complex points in the t_3 (^{1}H) period. 4 scans were recorded for each FID with an interscan delay of 1 s, which results in a total acquisition time of 36 hr.

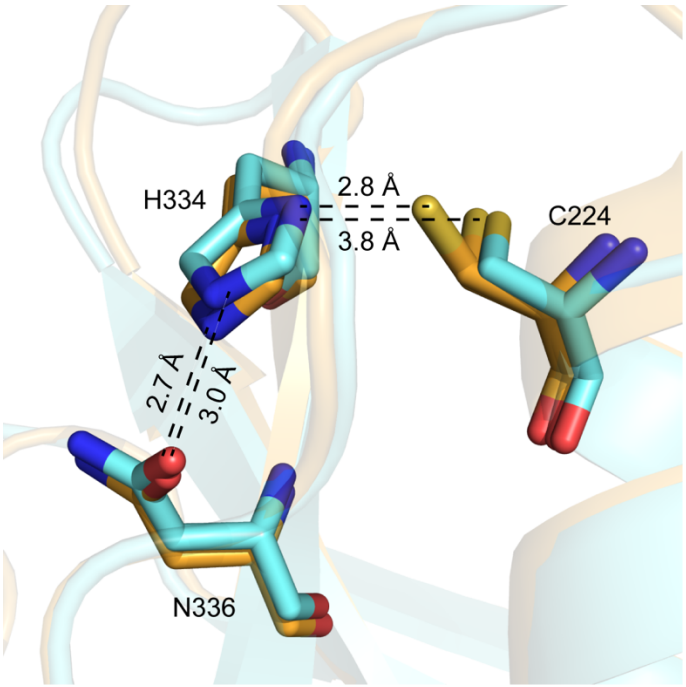

Figure S1. The comparison of the active sites in the crystal structures of the p-DUBA in the free form (carbon atoms in orange, PDB ID: 3PFY) and the p-DUBA covalently attached to ubiquitin-aldehyde (carbon atoms in cyan, PDB ID: 3TMP). In the free form, the catalytic cysteine displays two conformers with equal occupancy.

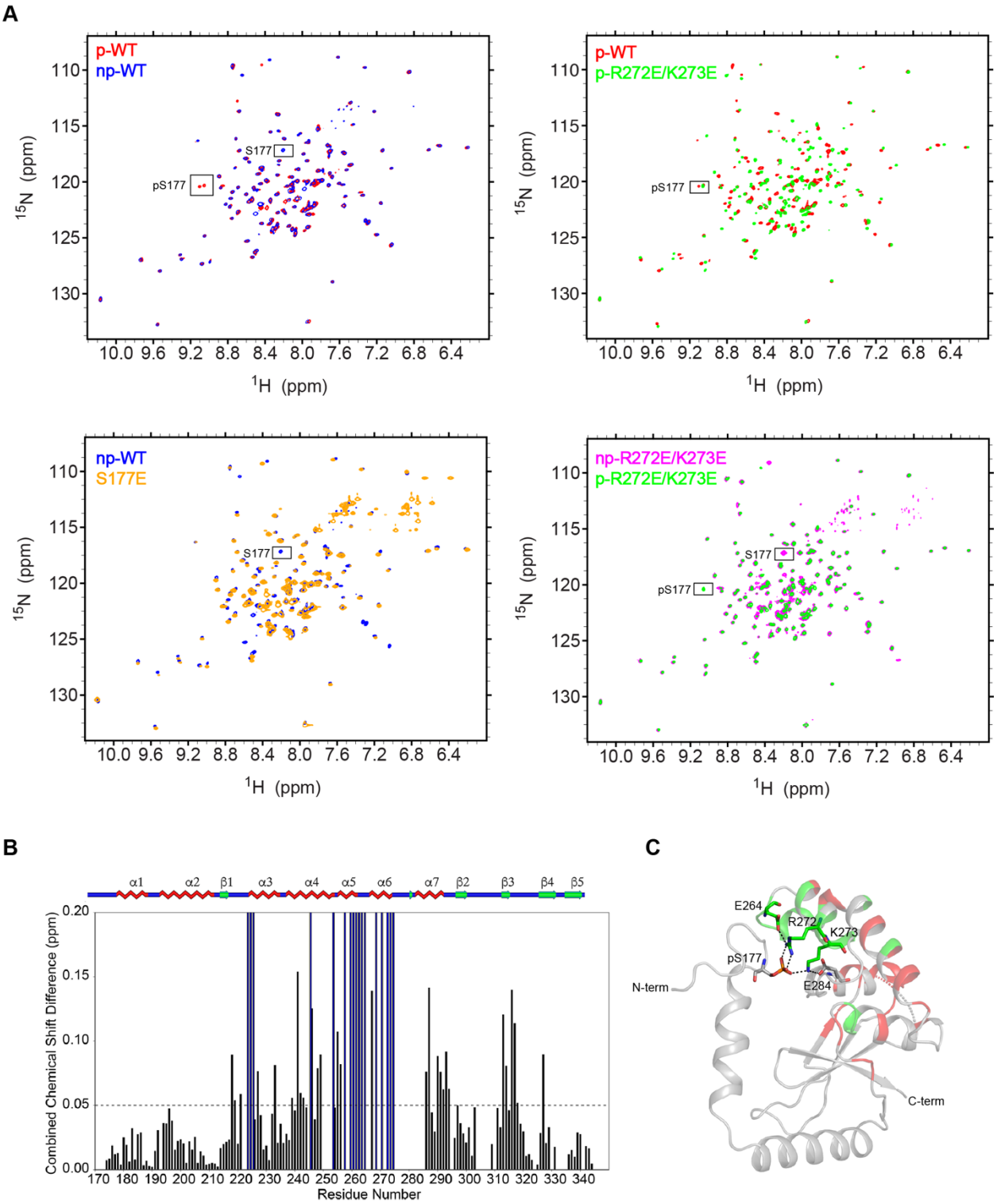

Figure S2. *A*, ^{15}N TROSY spectra of wild-type DUBA in phosphorylated (p-WT) and nonphosphorylated (np-WT) forms, R272E/K273E mutant in phosphorylated (p-R272E/K273E) and nonphosphorylated (np-R272E/K273E) forms, and S177E mutants of DUBA. The S177E mutant was ^{15}N-labeled and all the other forms of DUBA are [^{2}H, ^{15}N]-labeled. The data were acquired at 700 MHz ^{1}H frequency and 300 K. *B*, the combined chemical shift difference between the p-WT and the p-R272E/K273E mutant was calculated

using the equation $\Delta\delta_{diff} = \sqrt{\left(\Delta\delta_{H^N}^2 + \frac{\Delta\delta_N^2}{25}\right)/2}$ (7). The threshold for significant differences was set at $<\Delta\delta_{diff}> + 1\sigma$ (0.051 ppm) and indicated by the dashed line. Residues only detectable in the p-R272E/K273E mutant but not in the wild-type are represented by blue bars. $\Delta\delta_{diff}$ for these residues was set to an arbitrary value of 0.20 ppm. *C*, crystal structure of p-DUBA (PDB ID: 3TMP) with the residues showing combined chemical shift differences higher than the threshold highlighted in red and residues only detectable in the p-R272E/K273E mutant highlighted in green. The salt-bridge interactions of R272 and K273 with pS177 and other negatively charged residues nearby are highlighted with the stick representation.

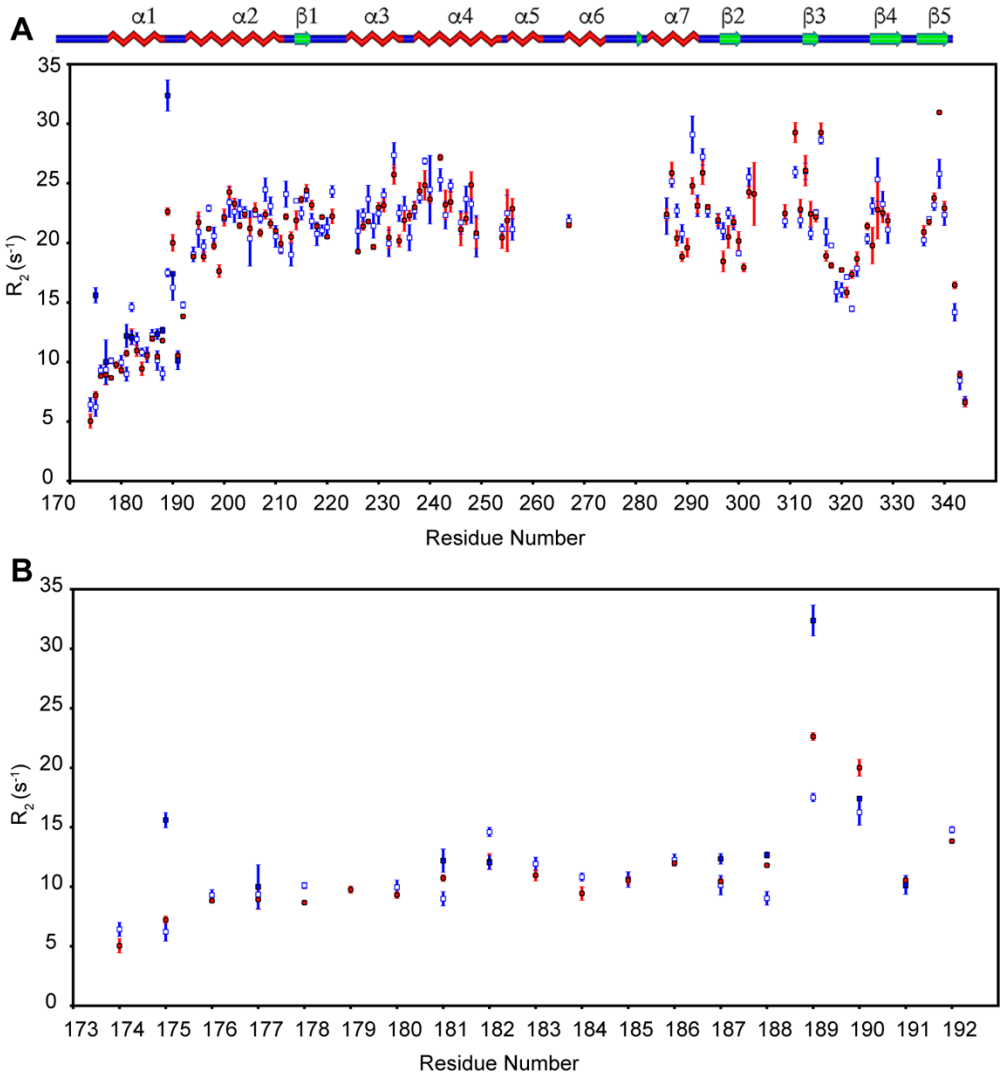

Figure S3. *A*, ^{15}N transverse relaxation rates (R_2) measured on np-DUBA (red) and p-DUBA (blue), with the open squares denoting the **a** conformer or the only conformer present, and the closed squares denoting the **b** conformer. *B*, the expanded view of residues 174-192. Data were acquired at 700 MHz ^{1}H frequency and 297.6 K.

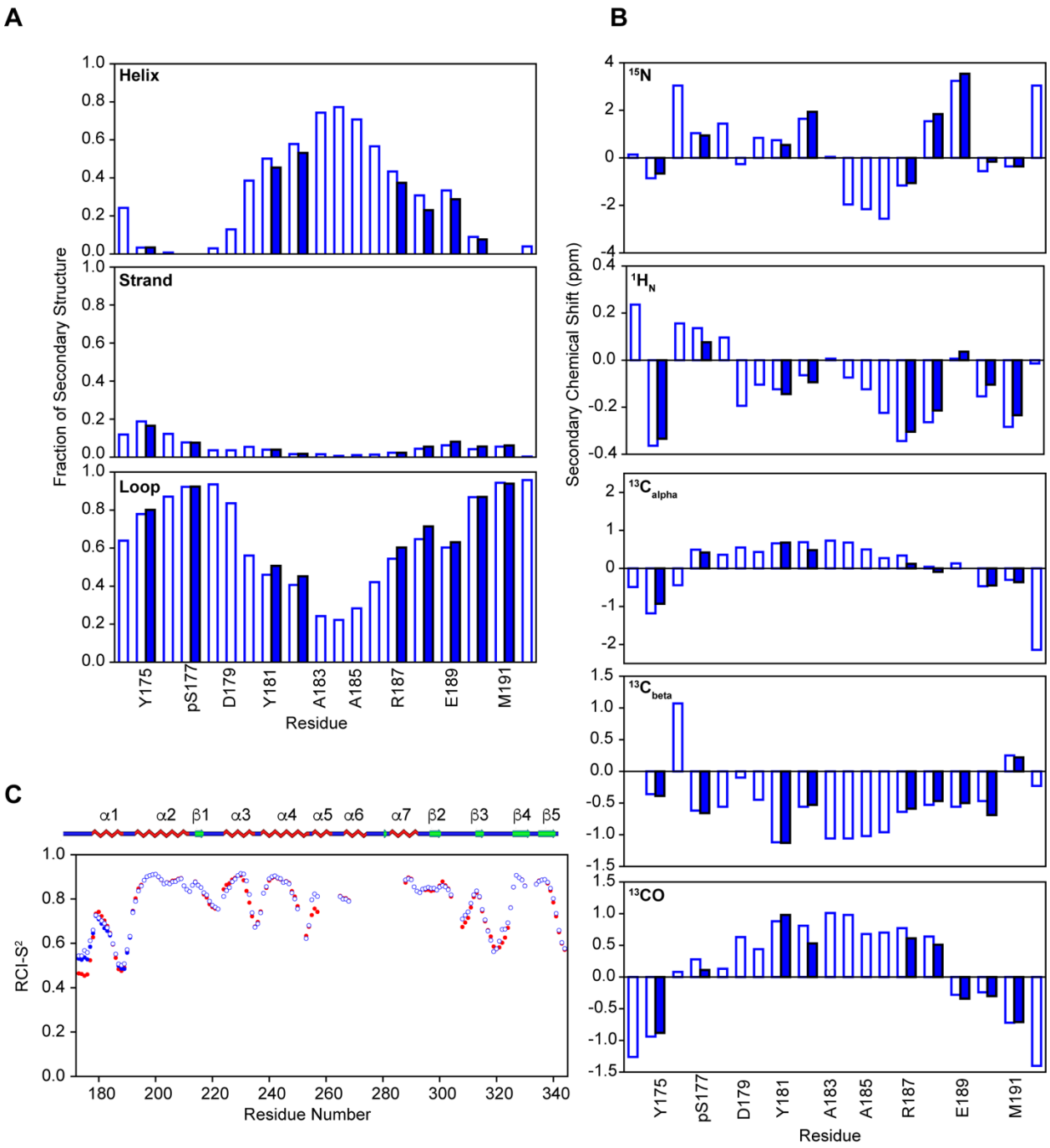

Figure S4. *A*, fractional secondary structures (helix, strand and loop) of residues 174-192 in p-DUBA predicted by TALOS-N (8). *B*, secondary chemical shifts of residues 174-192 in p-DUBA. Random coil shifts of all unmodified amino acids were from TALOS-N; for pSer, the random coil shifts were from the reference (9). The **a** conformer or the only conformer present is represented by open bars, and the **b** conformer by solid bars. *C*, backbone order parameters, RCI (random coil index)-S^2, of np-DUBA (red) and p-DUBA (blue) predicted by TALOS-N (8,10). Open circles represent the **a** conformer or the only conformer present, and the closed circles represent the **b** conformer. $^{13}C_\alpha$, $^{13}C_\beta$, ^{13}CO, ^{15}N and $^{1}H_N$ chemical shifts were used to obtain predictions by TALOS-N.

A

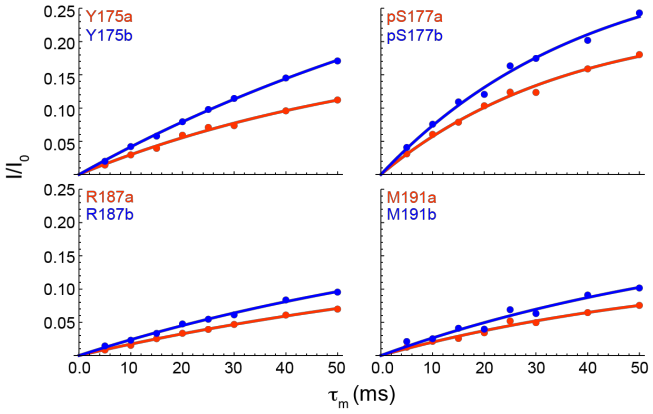

B

Residue	*k* (s^{-1})		$(k_b-k_a)/k_b$ [a]
	a conformer	**b** conformer	
G174	28.1 ± 0.7		
Y175	4.1 ± 0.2	5.52 ± 0.08	0.26
N176	8.03 ± 0.09		
S177	8.3 ± 0.3	10.5 ± 0.5	0.21
E178[b]	0.76 ± 0.02		
D179	n.d.[c]		
E180	0.57 ± 0.04		
Y181	2.2 ± 0.1	n.d.	
E182	0.90 ± 0.06	1.30 ± 0.04	0.31
A183	1.13 ± 0.04		
A184	2.30 ± 0.07		
A185	n.d.		
A186	1.48 ± 0.06		
R187	2.28 ± 0.06	3.2 ± 0.1	0.29
I188	1.18 ± 0.05	n.d.	
E189	n.d.	1.7 ± 0.2	
A190	1.8 ± 0.2	2.2 ± 0.2	0.18
M191	2.8 ± 0.2	3.6 ± 0.4	0.22

[a] k_a and k_b stand for the solvent exchange rates for the **a** and **b** conformers, respectively.
[b] The italic type denotes residues for which the data were fit using a linear model rather than the full equation.
[c] Values were not determined due to peak overlap.

Figure S5. *A*, representative build-up curves during the solvent exchange period from the CLEANEX experiment. *B*, rates of solvent exchange (*k*) for residues before helix α2 in the tabular format.

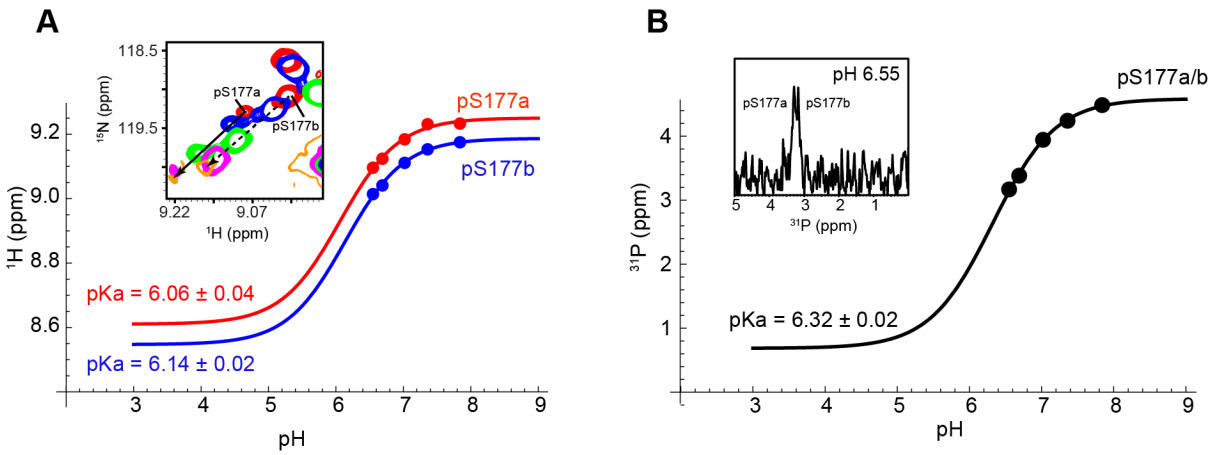

Figure S6. *A*, the pH titration curves of p-DUBA determined from the amide ^{1}H chemical shifts. The inset shows peak movement of pS177 as the pH value increases, as indicated by the arrows. The pH values are, 6.55 (red), 6.69 (blue), 7.02 (green), 7.36 (magenta) and 7.84 (orange). *B*, the pH titration curve of p-DUBA from the ^{31}P chemical shifts. For the 1D ^{31}P spectrum shown in the inset, an exponential apodization function corresponding to 5 Hz line broadening was applied to the time domain data before the Fourier transform. The **a** and **b** conformers are not well-resolved and were not analyzed separately. The titration curve was constructed from the averaged chemical shifts of the **a** and **b** conformers when they are partially resolved, or the chemical shift of the single peak observed.

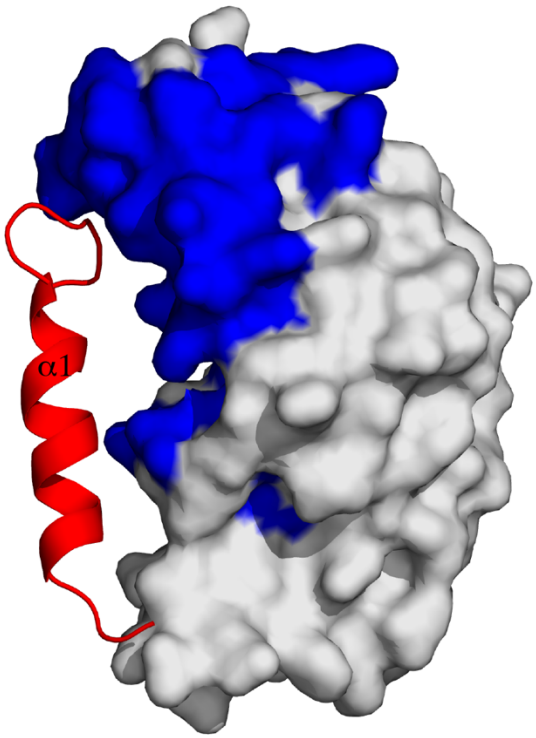

Figure S7. The p-DUBA crystal structure (PDB ID: 3TMP) with residues not visible in ^{15}N TROSY spectra highlighted in blue. Helix α1 and the α1-α2 loop (residues 172 – 193) are shown in cartoon representation and the remaining residues (194 – 340) in surface presentation.

Table S1. Secondary structure elements in crystal structures of the catalytic domain of DUBA

PDB ID: 3TMP (bound)[a]		PDB ID: 3PFY (free)	
secondary structure	residue number	secondary structure	residue number
α1	178-188	α1	not visible
α2	194-211	α2	194-211
β1	214-216	β1	214-216
α3	224-234	α3	224-234
α4	237-253	α4	237-253
α5	255-261	α5	255-258
α6	266-273	α6	not visible
α7	282-291	α7	282-292
β2	296-299	β2	296-299
β3	312-314	β3	312-314
β4	325-330	β4	325-330
β5	334-339	β5	334-339

[a] In this structure, p-DUBA is conjugated to ubiquitin-aldehyde through the active site cysteine, C224.

Table S2. ^{1}H and ^{15}N chemical shifts of residues 174-192 in various forms of DUBA[a]

	np-DUBA		p-DUBA		np-R272E/K273E		p-R272E/K273E		S177E	
residue	N (ppm)	H^N (ppm)	N (ppm)	H^N (ppm)	N (ppm)	H^N (ppm)	N (ppm)	H^N (ppm)	N (ppm)	H^N (ppm)
G174	109.0	8.35	109.6	8.46	109.1	8.36	109.5	8.45	109.2	8.41
Y175a	120.6	7.97	120.1	7.85	120.7	7.99	120.3	7.87	120.5	7.96
Y175b			120.3	7.88						
N176	121.9	8.45	122.4	8.47	122.1	8.41	122.3	8.45	122.1	8.43
S177a	117.1	8.20	120.5	9.14	117.2	8.20	120.3	9.07	-	-
S177b			120.4	9.08						
E178	122.8	8.50	122.3	8.39	122.8	8.49	122.2	8.39	122.3	8.40
D179	120.7	8.14	120.8	8.11	120.8	8.13	120.8	8.12	121.6	8.15
E180	121.6	8.15	121.7	8.19	122.0	8.18	121.9	8.18	121.6	8.15
Y181a	121.5	8.03	121.7	8.09	121.5	8.03	121.4	8.06	121.6	8.09
Y181b			121.5	8.07						
E182a	122.6	8.19	122.5	8.23	122.8	8.18	122.8	8.19	122.7	8.21
E182b			122.8	8.20						
A183	124.5	8.07	124.5	8.09	124.7	8.07	124.7	8.09	124.7	8.10
A184	122.5	7.97	122.5	8.01	122.6	7.98	122.5	8.01	122.6	8.00
A185	122.3	7.94	122.3	7.96	122.5	7.93	122.4	7.96	122.4	7.95
A186	122.0	7.87	121.9	7.86	122.1	7.88	122.1	7.87	122.0	7.87
R187a	120.0	7.88	120.0	7.86	120.2	7.90	120.1	7.90	120.1	7.88
R187b			120.1	7.90						
I188a	122.3	7.90	122.1	7.88	122.4	7.95	122.3	7.93	122.2	7.90
I188b			122.4	7.93						
E189a	124.2	8.31	124.1	8.30	124.5	8.34	124.4	8.34	124.3	8.32
E189b			124.4	8.33						
A190a	124.0	7.94	123.9	7.93	124.3	7.99	124.3	7.99	124.1	7.94
A190b			124.3	7.98						
M191a	119.9	7.95	119.9	7.94	119.9	7.99	119.8	8.00	119.9	7.95
M191b			119.9	7.99						
D192	124.0	8.28	124.1	8.29	124.1	8.26	124.0	8.26	124.1	8.29

[a] Chemical shifts were measured at 300 K. For both ^{1}H and ^{15}N nuclei, the chemical shifts of the TROSY components are reported. The chemical shifts corresponding to the **b** conformer in p-DUBA and the only conformer in p-R272E/K273E are highlighted in red for easy comparison.

Table S3. The relative volumes of cross-peaks from the **a** conformer in p-DUBA[a]

residue	relative peak volume (%) (Sample 1)	relative peak volume (%) (Sample 2)
S177a	50	49
E182a	56	58
R187a	58	59
I188a	65	65
E189a	69	73
A190a	63	64
M191a	63	63

[a]The volumes of cross-peaks corresponding to the **a** and **b** conformers were determined from two ^{15}N TROSY spectra recorded on two independently prepared samples to ensure reproducibility. The relative peak volume of the **a** conformer is represented as a percentage of the sum of the two conformers. Y175 and Y181 display two conformers but were excluded from the analysis because the cross-peaks partially overlap with other residues.

Table S4. Cα, Cβ and C' chemical shifts of residues 173-193 in p-DUBA[a]

residue	Cα (ppm)	Cβ (ppm)	C' (ppm)
A173	52.19	18.21	177.88
G174	44.61	-	173.64
Y175a	56.92	38.44	174.96
Y175b	57.17	38.41	175.02
N176	52.36	38.97	175.28
S177a	58.89	65.08	175.18
S177b	58.82	65.04	175.01
E178	56.76	29.14	176.73
D179	54.55	40.70	176.93
E180	56.83	29.25	177.04
Y181a	58.76	37.68	176.78
Y181b	58.78	37.67	176.88
E182a	57.09	29.14	177.41
E182b	56.88	29.17	177.13
A183	53.03	17.94	178.81
A184	52.98	17.94	178.78
A185	52.80	17.98	178.48
A186	52.57	18.04	178.50
R187a	56.44	29.66	177.07
R187b	56.22	29.71	176.91
I188a	61.34	37.47	177.04
I188b	61.21	37.53	176.91
E189a	56.53	29.14	176.32
E189b	56.40	29.20	176.26
A190a	51.83	18.53	177.56
A190b	51.85	18.31	177.50
M191a	55.00	32.85	175.58
M191b	54.94	32.82	175.59
D192	51.86	40.57	174.90
P193	64.38	31.26	178.28

[a] Chemical shifts were measured at 296 K and 700 MHz ^{1}H frequency. Correction for deuterium isotope shift was not applied.

Table S5. ^{1}H and ^{15}N line widths of cross-peaks from residues 174-192 of p-DUBA in an ^{15}N TROSY recorded at 299.6 K[a]

Residue[b]	^{1}H line width[c] (Hz)		^{15}N line width[d] (Hz)	
	a conformer	**b** conformer	**a** conformer	**b** conformer
G174	24		20	
N176	23		15	
S177	26	21	19	19
E178	13		10	
E180	13		10	
E182	15	14	11	14
A183	14		11	
A184	12		11	
A185	14		17	
A186	15		14	
R187	13	16	10	11
I188	17	17	12	11
E189	13	12	11	12
A190	15	19	13	13
M191	17	21	13	14
D192	14		11	

[a] Line widths that are significantly different between the **a** and **b** conformers are highlighted in red.
[b] Only residues yielding well-resolved cross-peaks are shown in the table.
[c] The digital resolution is 11.3 Hz for the ^{1}H dimension.
[d] The digital resolution is 10.6 Hz for the ^{15}N dimension.

References:

1. Hwang, T. L., van Zijl, P. C., and Mori, S. (1998) Accurate quantitation of water-amide proton exchange rates using the phase-modulated CLEAN chemical EXchange (CLEANEX-PM) approach with a Fast-HSQC (FHSQC) detection scheme. *J. Biomol. NMR* **11**, 221-226
2. Zhu, G., Xia, Y., Nicholson, L. K., and Sze, K. H. (2000) Protein dynamics measurements by TROSY-based NMR experiments. *J. Magn. Reson.* **143**, 423-426
3. Baryshnikova, O. K., Williams, T. C., and Sykes, B. D. (2008) Internal pH indicators for biomolecular NMR. *J. Biomol. NMR* **41**, 5-7
4. Maurer, T., and Kalbitzer, H. R. (1996) Indirect Referencing of 31P and 19F NMR Spectra. *J. Magn. Reson. B* **113**, 177-178
5. Croke, R. L., Patil, S. M., Quevreaux, J., Kendall, D. A., and Alexandrescu, A. T. (2011) NMR determination of pKa values in alpha-synuclein. *Protein Sci.* **20**, 256-269
6. Platzer, G., Okon, M., and McIntosh, L. P. (2014) pH-dependent random coil (1)H, (13)C, and (15)N chemical shifts of the ionizable amino acids: a guide for protein pK a measurements. *J. Biomol. NMR* **60**, 109-129
7. Grzesiek, S., Stahl, S. J., Wingfield, P. T., and Bax, A. (1996) The CD4 determinant for downregulation by HIV-1 Nef directly binds to Nef. Mapping of the Nef binding surface by NMR. *Biochemistry* **35**, 10256-10261
8. Shen, Y., and Bax, A. (2013) Protein backbone and sidechain torsion angles predicted from NMR chemical shifts using artificial neural networks. *J. Biomol. NMR* **56**, 227-241
9. Hendus-Altenburger, R., Fernandes, C. B., Bugge, K., Kunze, M. B. A., Boomsma, W., and Kragelund, B. B. (2019) Random coil chemical shifts for serine, threonine and tyrosine phosphorylation over a broad pH range. *J. Biomol. NMR* **73**, 713-725
10. Berjanskii, M. V., and Wishart, D. S. (2005) A simple method to predict protein flexibility using secondary chemical shifts. *J. Am. Chem. Soc.* **127**, 14970-14971